

## Interactions of the $\eta$ meson in the nuclear medium and eta-nuclear bound states

---

**Jiří Mareš\*, Aleš Cieplý**

*Nuclear Physics Institute, 250 69 Rez, Czech Republic*

*E-mail: [mares@ujf.cas.cz](mailto:mares@ujf.cas.cz)*

**Nir Barnea, Eli Friedman, Avraham Gal**

*Racah Institute, The Hebrew University, Jerusalem 91904, Israel*

We report on our recent calculations of  $\eta$ -nuclear quasi-bound states using energy-dependent  $\eta N$  scattering amplitudes derived within coupled-channel models that incorporate the  $N^*(1535)$  resonance. The role played by strong energy and density dependence of the scattering amplitudes and the implications of self-consistent treatment are discussed.

*The 26th International Nuclear Physics Conference*

*11-16 September, 2016*

*Adelaide, Australia*

---

\*Speaker.

## 1. Introduction

The  $\eta N$  attraction near threshold seems to be strong enough to allow binding of the  $\eta$  meson in nuclei. However, strong energy dependence and in-medium modifications of the  $\eta N$  scattering amplitudes, derived within coupled-channel models that capture the nature of the  $N^*(1535)$  resonance, have to be carefully taken into account in any reliable calculation.

The present contribution reports on systematic treatment of the energy and density dependences of the underlying  $\eta N$  scattering amplitudes in dynamical self-consistent calculations of  $\eta$  quasi-bound states in nuclei (more details can be found in Refs. [1, 2, 3]).

In Section 2, we discuss model dependence and in-medium modifications of the  $\eta N$  scattering amplitudes, introduce methods for calculating  $\eta$ -nuclear states in few- as well as many-body systems, and demonstrate how to incorporate the strong energy dependence of the scattering amplitudes near threshold in calculations of  $\eta$ -nuclei. In Section 3, we present selected results of our study of  $\eta$ -nuclear quasi-bound states and a brief summary is given in Section 4.

## 2. Methodology

The  $\eta N$  interaction has been described within coupled-channel models that fit or, in addition, generate dynamically the  $N^*(1535)$  resonance lying  $\approx 50$  MeV above the  $\eta N$  threshold. However, the derived  $\eta N$  scattering amplitudes exhibit appreciable model dependence, particularly at threshold and further down to subthreshold region which is relevant to calculations of  $\eta$ -nuclear quasi-bound states. This is illustrated in Fig. 1, where we present comparison of  $\eta N$  scattering amplitudes for three selected meson-baryon interaction models GW [4], CS [5], and GR [6].

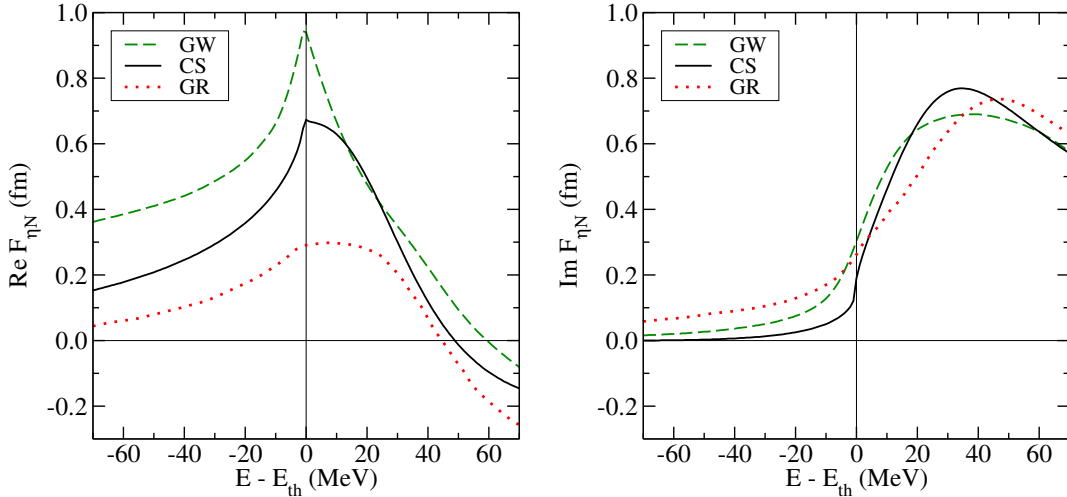


**Figure 1:** Energy dependence of the real (left panel) and imaginary (right panel) parts of the free  $\eta N$  scattering amplitude in interaction models GW [4] (dashed), CS [5] (solid), and GR [6] (dotted). The vertical line denotes the  $\eta N$  threshold.

The strong energy dependence of the  $\eta N$  scattering amplitudes has to be treated self-consistently. The argument  $\sqrt{s}$  in the scattering amplitudes is given by

$$\sqrt{s} = \sqrt{(\sqrt{s_{\text{th}}} - B_\eta - B_N)^2 - (\vec{p}_\eta + \vec{p}_N)^2} \leq \sqrt{s_{\text{th}}}, \quad (2.1)$$

where  $\sqrt{s_{\text{th}}} \equiv m_\eta + m_N$ , and  $B_\eta$  and  $B_N$  are  $\eta$  and nucleon binding energies, respectively. In the nuclear medium the momentum dependent term causes additional downward energy shift, since  $(\vec{p}_\eta + \vec{p}_N)^2 \neq 0$ . The energy shift can be approximated as [2]

$$\delta\sqrt{s} = \sqrt{s} - \sqrt{s_{\text{th}}} \approx -B_N \frac{\rho}{\rho_0} - \xi_N B_\eta \frac{\rho}{\rho_0} - \xi_N T_N \left(\frac{\rho}{\rho_0}\right)^{2/3} - \xi_\eta \frac{\sqrt{s}}{\omega_\eta E_N} 2\pi \text{Re} F_{\eta N}(\sqrt{s}, \rho) \rho, \quad (2.2)$$

where  $\xi_{N(\eta)} = m_{N(\eta)}/(m_N + m_\eta)$ ,  $\bar{\rho}$  is the average nuclear density,  $T_N = 23.0$  MeV at  $\rho_0$ , and  $B_N \approx 8.5$  MeV is the average nucleon binding energy. It is to be noted that for attractive scattering amplitudes, all terms in Eq. 2.2 are negative definite, providing substantial downward energy shift.

A variant of Eq. 2.2 was used in  $\eta$ -nuclear three- and four-body calculations [3]:

$$\delta\sqrt{s} = -\frac{B}{A} - \frac{A-1}{A} B_\eta - \xi_N \frac{A-1}{A} \langle T_{NN} \rangle - \xi_\eta \left(\frac{A-1}{A}\right)^2 \langle T_\eta \rangle, \quad (2.3)$$

where  $B$  is the total binding energy of the system,  $T_\eta$  is the kaon kinetic energy operator in the total cm frame and  $T_{NN}$  is the pairwise  $NN$  kinetic energy operator in the  $NN$  pair cm system (see [3] for details).

Few-body  $\eta NN$  and  $\eta NNN$  systems were calculated using variational method within a hyperspherical basis. For the  $NN$  interaction, the Minnesota central potential [7] and the Argonne AV4' potential [8] were used. The  $\eta N$  interaction was described by energy dependent local  $\eta N$  potentials that reproduce the  $\eta N$  scattering amplitudes below threshold in CS and GW interaction models [3]. The conversion widths were evaluated through the expression

$$\Gamma/2 \approx \langle \Psi_{\text{g.s.}} | -\text{Im} V_{\eta N} | \Psi_{\text{g.s.}} \rangle,$$

where  $V_{\eta N}$  sums over all pairwise  $\eta N$  interactions.

The interaction of the  $\eta$  meson with a nuclear many-body system was described by the Klein-Gordon (KG) equation of the form

$$[\nabla^2 + \tilde{\omega}_\eta^2 - m_\eta^2 - \Pi_\eta(\omega_\eta, \rho)] \psi = 0, \quad (2.4)$$

where  $\tilde{\omega}_\eta = \omega_\eta - i\Gamma_\eta/2$  is complex energy of  $\eta$ ,  $\omega_\eta = m_\eta - B_\eta$ , and  $\Gamma_\eta$  is the width of the  $\eta$ -nuclear bound state. The self-energy operator  $\Pi_\eta(\sqrt{s}, \rho) \equiv 2\omega_\eta V_\eta = -(\sqrt{s}/E_N) 4\pi F_{\eta N}(\sqrt{s}, \rho) \rho$  was constructed self-consistently using a relevant in-medium  $\eta N$  scattering amplitude  $F_{\eta N}(\sqrt{s})$  and RMF density of the core nucleus.

Several in-medium  $\eta N$  amplitudes  $F_{\eta N}(\sqrt{s}, \rho)$ , such as the GW amplitude, which were used in our many-body self-consistent calculations were obtained from the free-space amplitudes by applying a multiple scattering approach [9] (see Ref. [2] for details). In the chirally inspired

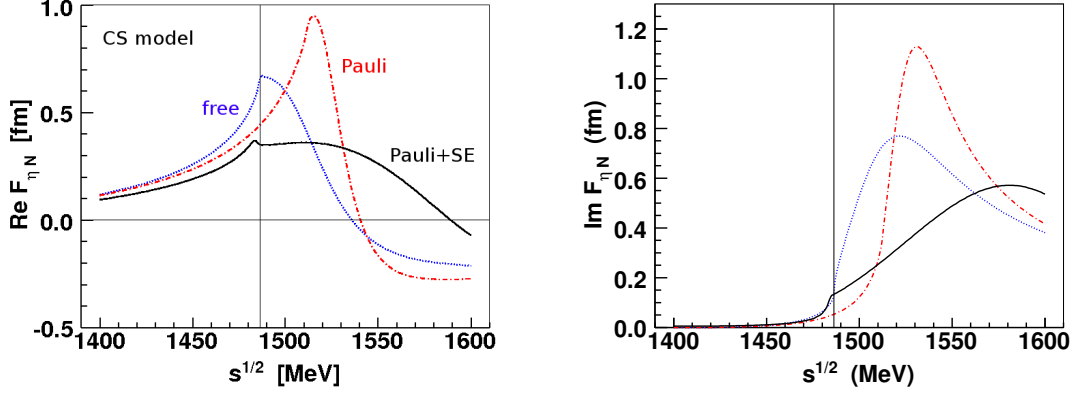


**Figure 2:** Real (left) and imaginary (right) parts of the  $\eta N$  scattering amplitude in CS model [5]. Dotted line: free space amplitude; dot-dashed: Pauli-blocked in-medium amplitude for  $\rho_0 = 0.17 \text{ fm}^{-3}$ ; solid: in-medium amplitude including hadron self-energies.

meson-baryon interaction models CS and GR, the Pauli principle restricts integration domain in the in-medium Green's function which enters the underlying Lippmann-Schwinger (Bethe-Salpeter) equations [2] (denoted 'Pauli'). Moreover, hadron self-energy insertions reflecting in-medium modifications could be included in the in-medium Green's function, as well (denoted 'Pauli+SE').

In Fig. 2, we demonstrate the nuclear medium effect on the energy dependence of the  $\eta N$  CS scattering amplitude. The peak structure observed for  $\text{Im}F_{\eta N}$  is related to the  $N^*(1535)$  resonance, generated dynamically in this model. In-medium Pauli blocking (dot-dashed line) shifts the peak to higher energies, while implementation of hadron self-energies (solid line) spreads the resonance structure over a broad energy region and practically dissolves it in the nuclear medium. The in-medium amplitudes decrease rapidly in going to the subthreshold energies relevant for  $\eta$ -nuclear quasi-bound states calculations and become weaker than the respective free-space amplitude. For instance, the relatively large value of the real part of the free-space amplitude at threshold is almost halved at nuclear matter density when hadron self-energies are included (Pauli+SE option). Taking into account in-medium hadron self-energies results in 2–3 MeV lower binding energies of calculated  $\eta$ -nuclear states than in the case of pure Pauli blocking (Pauli).

It is to be stressed that  $\text{Re}F_{\eta N}(\sqrt{s})$  and  $B_\eta$  appear as arguments in the expression for  $\delta\sqrt{s}$  (Eq. 2.2), which in turn serves as an argument for  $F_{\eta N}$  and thus for the self-energy  $\Pi_\eta$ . Therefore, a self-consistency scheme in terms of both  $\Pi_\eta$  and  $B_\eta$  is required in calculations. Another self-consistent scheme is required when hadron self-energies are taken into account, because the  $\eta$  self-energy  $\Pi_\eta$  appears in the in-medium Green's function which enters Lippmann-Schwinger equations used in the evaluation of  $\Pi_\eta$ .

### 3. Results

Our few-body calculations within the considered coupled-channel models CS and GW found *no* bound state solution for the  $\eta NN$  three-body system. For  $\eta NNN$  system, a weakly bound state was found for one particular variant of the  $\eta N$  potential that reproduced the GW scattering am-

$NN$ int.	$E(NNN)$	$\delta\sqrt{s_{sc}}$	$E_{gs}^{sc}$	$E_{\eta}^{sc}$	$\Gamma_{gs}^{sc}$
MN	-8.38	-13.52	-9.33	0.95	3.3
AV4'	-8.99	-15.83	-9.03	0.04	2.4

**Table 1:** Results of  $\eta NNN$  bound state calculations within the GW model. Energies and widths are in MeV.

plitudes. (see Ref. [3] for details). The results of calculations for both MN and AV4' models are shown in Table 1. The  $3N$  binding energies  $E(NNN)$  and self-consistent values of  $\delta\sqrt{s}$  are listed in the second and third column, respectively. The self-consistently evaluated energy shift  $\delta\sqrt{s}$  together with the energy dependence of the  $\eta N$  potential resulted in considerably reduced values of less than 1 MeV for the  $\eta$  separation energy  $E_{\eta}^{sc}$ . The  $\eta$  separation energies evaluated at threshold are between 2 – 3 MeV. The corresponding widths shown in the last column are relatively small.<sup>1</sup> It is to be noted that *no*  $\eta NNN$  bound states were found using more realistic  $NN$  interaction models.

In Fig. 3, we present the downward energy shift  $\delta\sqrt{s} = E - E_{th}$  as a function of the relative nuclear density  $\rho/\rho_0$  in Ca, evaluated self-consistently according to Eq. (2.2) for the CS and GW models (Pauli option). The energy shift at the central density ranges within  $55 \pm 10$  MeV and is about twice larger than  $\delta\sqrt{s}$  considered in previous calculations. The shift for the GW model exceeds that for the CS model due to stronger  $ReF_{\eta N}(\sqrt{s})$ .

It is instructive to compare our self-consistency scheme of calculating  $\eta$ -nuclear states using  $\delta\sqrt{s}$  of Eq. (2.2) with a  $\delta\sqrt{s} = -B_{\eta}$  self-consistency requirement applied in Ref. [6]. Figure 4 shows such comparison for the in-medium GR amplitude (Pauli+SE): our self-consistency scheme (marked  $\delta\sqrt{s}$ ) reduces considerably the GR binding energies and widths with respect to the original

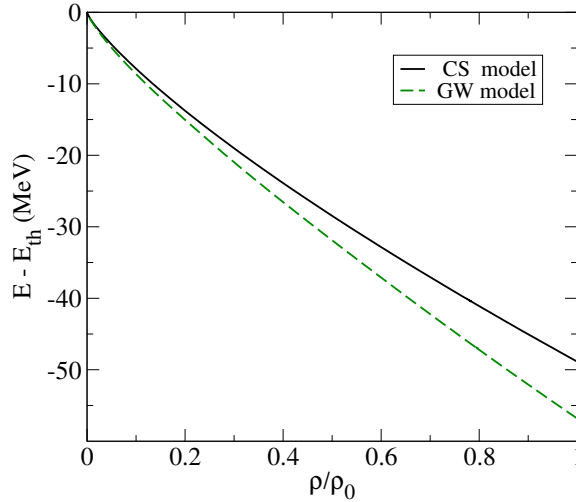


**Figure 3:** Subthreshold  $\eta N$  energies probed by the  $\eta$  nuclear potential as a function of the relative nuclear RMF density in Ca. Each of the two curves was calculated self-consistently for a particular  $\eta N$  subthreshold amplitude model.

<sup>1</sup>We found an error in normalization which made the originally calculated widths presented in Table 2 of Ref. [3] much larger.

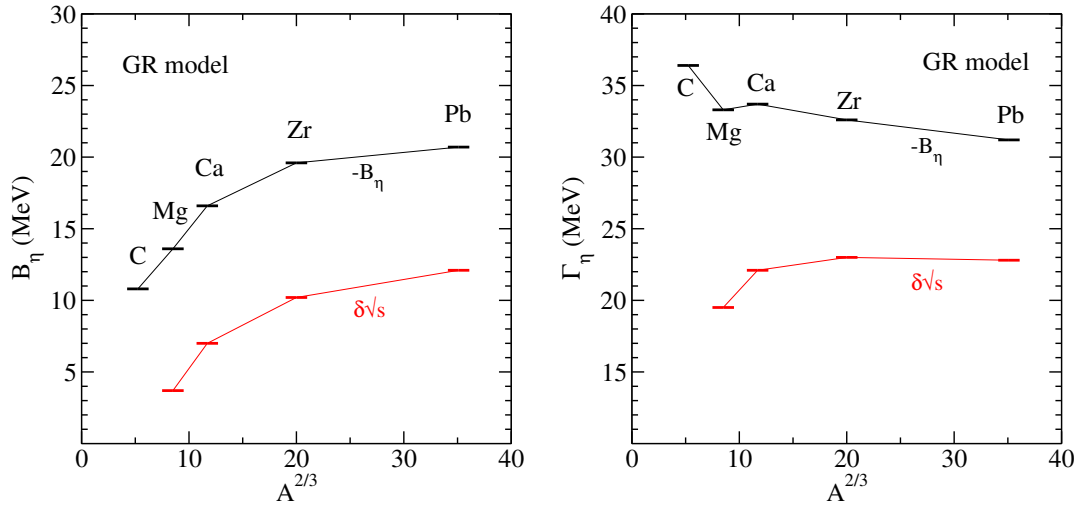


**Figure 4:** Binding energies (left) and widths (right) of the  $1s$   $\eta$ -nuclear states in selected nuclei calculated using the GR  $\eta N$  scattering amplitude [6] with different procedures for subthreshold energy shift  $\delta\sqrt{s}$ .

calculations of Ref. [6] that used  $\delta\sqrt{s} = -B_\eta$  (marked  $-B_\eta$ ). However, even the considerably reduced GR widths are still too large, which suggests that it would be extremely difficult to resolve  $\eta$ -nuclear states in such a case.

The model dependence of the  $\eta N$  scattering amplitudes shown in Fig. 1 manifests itself in the calculations of  $\eta$ -nuclear states. Fig. 5 presents binding energies  $B_\eta$  and widths  $\Gamma_\eta$  calculated for the  $1s$   $\eta$ -nuclear states in selected nuclei using the  $\eta N$  CS and GW amplitudes (the results for the GR model are shown in Fig. 4).

The left panel of Fig. 5 demonstrates that for both  $\eta N$  amplitude models the binding energy

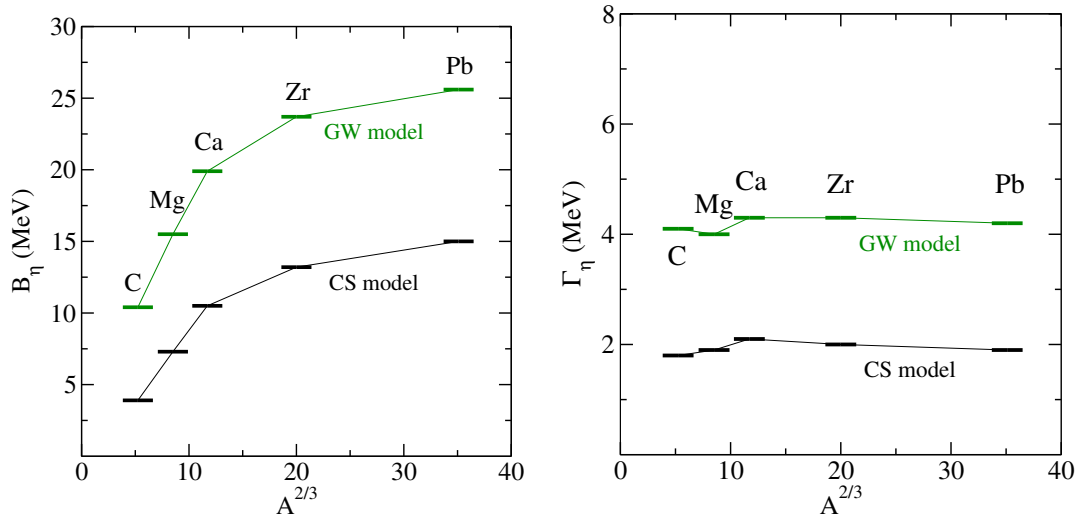


**Figure 5:** Binding energies (left) and widths (right) of  $1s$   $\eta$ -nuclear states in selected nuclei calculated self-consistently using the CS and GW  $\eta N$  scattering amplitudes.

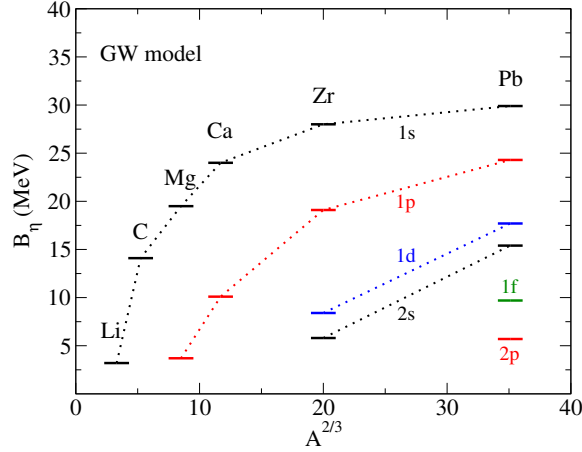


**Figure 6:** Spectra of  $\eta$ -nuclear bound states across the periodic table, calculated self-consistently using the GW  $\eta N$  scattering amplitudes.

increases with  $A$  and tends to saturate for large values of  $A$ . The hierarchy of the binding energies  $B_\eta$  calculated within considered  $\eta N$  amplitude models reflects the strength of  $\text{Re}F_{\eta N}$  in the sub-threshold region (see Fig. 1). Among the models presented here, the GR model yields the least binding of the  $\eta$  meson in considered nuclei. On the other hand,  $\text{Re}F_{\eta N}(\sqrt{s})$  of the CS model is strong enough to bind  $\eta$  in  $^{12}\text{C}$ , and the GW model yields  $\eta$  quasi-bound states even in much lighter nuclei – it predicts the  $1s$   $\eta$ -nuclear bound state in the  $\eta NNN$  system, as shown in Table 1.

The calculated widths  $\Gamma_\eta$  are presented in the right panel of Fig. 5. The CS and GW models yield remarkably small uniform widths of order 2 and 4 MeV, respectively. However, the GR model predicts much larger widths which increase with  $A$ , as shown in Fig. 5. This reflects partly the energy dependence of  $\text{Im}F_{\eta N}(\sqrt{s})$  in the subthreshold region and partly the differences in the downward energy shifts. For instance, large  $\delta\sqrt{s}$  in the GW model (57 MeV at  $\rho_0$  in Ca) causes a particularly large reduction in the strength of  $\text{Im}F_{\eta N}(\sqrt{s})$ .

Finally, in Fig. 6 we present  $\eta$ -nuclear single-particle spectra across the periodic table, calculated self-consistently using the GW model. These dynamical calculations include Pauli blocking evaluated in the multiple scattering approach [9].

The widths calculated here do not include contributions from two-nucleon processes which are estimated to add a few MeV. We may therefore conclude that  $\eta$ -nuclear states could in principle be observed if the CS and GW models turn out to be realistic ones. Other models considered by us (GR [6], M1 and M2 [10], and KSW [11]) give either too large widths or are too weak to generate  $\eta$ -nuclear bound states in lighter nuclei.

#### 4. Conclusions

In this contribution, we reported on our recent self-consistent calculations of  $\eta$ - nuclear quasi-bound states using  $\eta N$  scattering amplitudes constructed within meson-baryon coupled-channel models. We focused on the role played by the underlying meson-baryon subthreshold dynamics. The subthreshold  $\eta N$  amplitudes relevant for calculations of  $\eta$  nuclear bound states are substan-

tially weaker than these amplitudes at threshold. The relatively large downward energy shift in our self-consistent approach leads to bound state energies and widths which are considerably smaller than those evaluated in other comparable approaches. The small widths calculated in the CS and GW models might encourage further experimental searches for  $\eta$  nuclear bound states. However, calculated widths (as well as binding energies) of  $\eta$ -nuclear quasi-bound states are strongly model dependent – other models predict widths substantially larger. To date, the only claim of observing an  $\eta$  nuclear bound state is in the reaction  $p + {}^{27}\text{Al} \rightarrow {}^3\text{He} + {}^{25}_{\eta}\text{Mg} \rightarrow {}^3\text{He} + p + \pi^- + X$  reported by the COSY-GEM collaboration [12].

## Acknowledgments

This work was supported by the GACR Grant No. P203/15/04301S.

## References

- [1] E. Friedman, A. Gal, J. Mareš, *Phys. Lett. B* **725** (2013) 334.
- [2] A. Cieplý, E. Friedman, A. Gal, J. Mareš, *Nucl. Phys. A* **925** (2014) 126.
- [3] N. Barnea, E. Friedman, A. Gal, *Phys. Lett. B* **747** (2015) 345.
- [4] A.M. Green, S. Wycech, *Phys. Rev. C* **71** (2005) 014001.
- [5] A. Cieplý, J. Smejkal, *Nucl. Phys. A* **919** (2013) 46.
- [6] T. Inoue, E. Oset, *Nucl. Phys. A* **710** (2002) 354; C. García-Recio, T. Inoue, J. Nieves, E. Oset, *Phys. Lett. B* **550** (2002) 47.
- [7] D. R. Thomson, M. LeMere, Y. C. Tang, *Nucl. Phys. A* **286** (1977) 53.
- [8] R. B. Wiringa, S. C. Pieper, *Phys. Rev. C* **89** (2002) 182501.
- [9] T. Wass, M. Rho and W. Weise, *Nucl. Phys. A* **617** (1997) 449.
- [10] M. Mai, P.C. Bruns, U.-G. Meissner, *Phys. Rev. D* **86** (2013) 015201.
- [11] N. Kaiser, P. B. Siegel, W. Weise, *Phys. Lett. B* **362** (1995) 23.
- [12] A. Budzanowski, et al. (COSY-GEM Collaboration), *Phys. Rev. C* **79** (2009) 012201(R).